Effects of Abrupt Changes in Film Thickness on Magnetic Bubble Forces

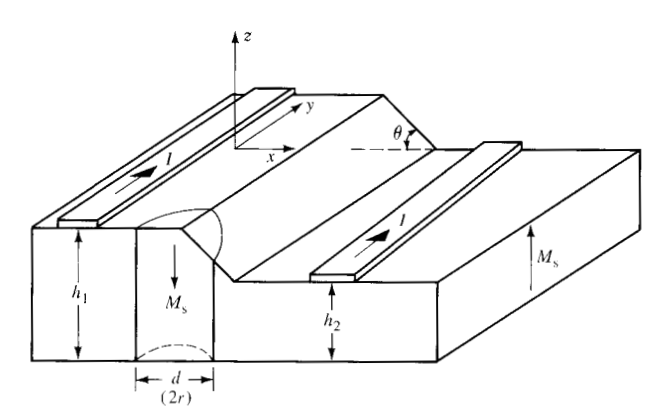
Abstract: Forces on a magnetic bubble due to abrupt asymmetric changes in the surface configuration of the magnetic film are investigated theoretically and experimentally. A model is derived for calculating the forces on a bubble as it is being moved by conductor propagation through a thickness gradient in the film. An experiment is described in which the forces necessary to move a bubble through this transition region are measured and compared with predicted values computed from the model. Results are presented for a 20° gradient with a cut 0.62 µm deep in a garnet film, nominally 3.8 µm thick, prepared by liquid phase epitaxy.

Introduction

In a study of the stability of a magnetic bubble when it interacts with topological elements such as dams, grooves, and gradient transitions from thick to thin regions, it is essential to calculate the forces on the bubble due to these barriers and transition regions.

Thiele et al. [1] calculated the general translation forces on a bubble due to various gradients in film thickness, material composition, and temperature. Their analysis, however, may be considered a small-signal variational approach in that all variables were assumed to be independent and all variations were small. This eliminates the case where, for example, the film thickness changes abruptly over the bubble diameter, and this

Figure 1 Section of magnetic bubble film, showing thickness gradient.



abrupt variation creates a gradient in the internal magnetic field that must be accounted for.

In a recent publication, Druyvesteyn [2] rigorously analyzed the problem for abrupt changes in thickness, in which the variations were symmetrical about the center of the material. In the case discussed here, however, the thickness changes occur only on the upper surface of the bubble material. The results presented in this paper, nevertheless, are in qualitative agreement with those of Druyvesteyn.

Analysis

The system that is analyzed is illustrated in Fig. 1. It consists of a uniformly magnetized garnet film with a gradient transition region separating the portions of different thickness, a cylindrical bubble domain, and a pair of current conductors on the surface of the film on each side of the slope. The current in the pair of conductors applies a force to the bubble that moves it down the slope from the thicker region to the thinner one and vice versa. The existence of the gradient itself and the fact that the bubble is changing its effective height and diameter exert translational forces on the bubble in addition to the applied force. Because determining the force due to the applied current in the pair of conductors is a straightforward procedure, we concentrate on those additional forces that arise.

We begin by viewing the system in Fig. 1 as a superposition of a sloped platelet with uniform magnetization M_s in the z direction and a cylindrical domain with magnetization of $2M_s$ in the -z direction. The total energy

of the system consists of the demagnetizing energy $E_{\rm m}$, the domain wall energy $E_{\rm w}$, and the external bias field energy $E_{\rm H}$. The value $E_{\rm m}$ can be derived by using the method of Cape and Lehman [3]. The total demagnetizing energy is given as

$$E_{\rm m} = \int \mu_{\rm 0} M_{\rm s} H_{\rm v} dv + \int 2\mu_{\rm 0} M_{\rm s} H_{\rm p} dv - \frac{1}{2} \int \mu_{\rm 0} M_{\rm s} H_{\rm p} dV_{\rm p}, \tag{1}$$

where $H_{\rm v}$ is the z component of the demagnetizing field of the bubble, $H_{\rm p}$ is the z component of the platelet field, v is the volume of the bubble domain, and $V_{\rm p}$ is the volume of the platelet.

The last term in (1) is just the saturation energy of the platelet itself. Because we are interested in the change in $E_{\rm m}$ with respect to the saturated platelet, we write

$$\Delta E_{\rm m} = \int \mu_0 M_{\rm s} H_{\rm v} dv + \int 2\mu_0 M_{\rm s} H_{\rm p} dv. \tag{2}$$

Equation (2) is in a convenient form for this particular problem. It separates out the platelet field term $H_{\rm p}$ which, in this case, is not independent of position, as it is in the case of a platelet of constant thickness, and must be computed separately as a function of position. The quantity $E_{\rm H}$ is simply given as

$$E_H = \int 2\mu_0 M_{\rm s} H_{\rm a} dv,\tag{3}$$

where $H_{\rm a}$ is the applied bias field, plus any other externally applied field such as the field due to the current in the conductor overlay. Finally, $E_{\rm w}$ is given as

$$E_{\rm w} = \int \sigma_{\rm w} dA_{\rm w},\tag{4}$$

where $\sigma_{\rm w}$ is the domain wall energy per unit area and $A_{\rm w}$ is the area of the domain wall.

Adding (2), (3), and (4), we have

$$\Delta E_{\mathrm{T}} = \int \mu_0 M_{\mathrm{s}} H_{\mathrm{v}} dv + \int 2\mu_0 M_{\mathrm{s}} H_{\mathrm{p}} dv + \int 2\mu_0 M_{\mathrm{s}} H_{\mathrm{a}} dv + \int \sigma_{\mathrm{w}} dA_{\mathrm{w}}.$$
 (5)

The translational force F_t can then be found from (5) as

$$\mathbf{F}_{\star} = -\nabla(\Delta E_{\mathrm{T}}). \tag{6}$$

Because the platelet is not of uniform thickness, the variables $H_{\rm v}$, $H_{\rm p}$, v, and $A_{\rm w}$ are all functions of position of the center of the bubble domain. In addition, $\Delta E_{\rm T}$ must be minimized at each position to maintain equilibrium of the radial forces [4]. Therefore, to avoid the complexity of a three-dimensional potential and a minimization problem, we make the following assumptions:

- 1. The base of the bubble domain remains circular.
- 2. For gentle slopes, the demagnetizing energy for the segmented cylinder (Fig. 1) can be found from a right circular cylinder whose height gives the same volume as the segmented cylinder.

Averaging the fields over the volume of the bubble, we express (6) as

Table 1. Film parameters used for the model based on Figure 1.

Symbol	Definition	Value
$4\pi M_{\circ}$	Saturation magnetization	13.85 kA/m
1 "	Characteristic length	$0.62~\mu m$
h_1	Thickness of thick region	$3.77 \mu m$
$h_1 h_2$	Thickness of thin region	$3.15 \mu m$
Θ́	Gradient angle	20°

$$F_{t} = -\frac{\pi r \mu_{0} M_{s}}{2} \left[\hat{H}_{v} + 2(\hat{H}_{p} + \hat{H}_{a}) + \frac{2\sigma_{w}}{r \mu_{0} M_{s}} \right] \Delta h$$
$$-\frac{\pi r \mu_{0} M_{s}}{2} \left[\Delta H_{v} + 2(\Delta H_{p} + \Delta H_{a}) \right] h, \tag{7}$$

where the ΔH quantities and Δh represent differences taken across the bubble, and r is the bubble domain radius obtained by minimizing the total energy at the given position of the bubble. Note that, if $H_{\rm p}$ is constant, i.e., the platelet is of uniform thickness, Eq. (7) reduces to Eq. (11) of Ref. 1.

Equation (7) indicates that there are two components of the force—one due to the thickness gradient, ∇h , and the other due to the field gradient, ∇H . As pointed out by Thiele et al. [1], in the range of stable bubble operation the sign of the coefficient of Δh in (7) is such that the force due to the thickness change is in the direction of the thickness gradient. However, for abrupt changes in thickness over a distance comparable to the bubble diameter, it is shown here that the increment, Δh , creates a change in platelet field, ΔH_p , which generates a force that is directed opposite to the thickness gradient. The net force may, therefore, be in either direction, depending on which component of (7) is dominant. This fact was also pointed out by Druyvesteyn [2].

Results for small-angle gradient

Although we have obtained results for a number of geometric configurations, we concentrate on the one shown in Fig. 1. Because the purpose of this configuration is to transport a bubble from the thick region to the thinner one, we present data for small angles only. Large-angle slopes tend to be efficient barriers and it is very difficult to transport bubbles across them. Unless otherwise stated, the material parameters are those given in Table 1.

The first step in the analysis is to compute the fields created by the change in thickness. Figure 2 displays H_z and H_x averaged through the material for the profile shown. The 20° slope generates a change in H_z of about $8.8 \times 10^2 \text{A/m}$ (12 Oe) from the top of the slope to the bottom and about $8.4 \times 10^2 \text{ A/m}$ in-plane field H_x . The quantity H_p is identically equal to H_z in Fig. 2. H_p is equal to $-M_s$ at $x = \pm \infty$ and varies somewhat above

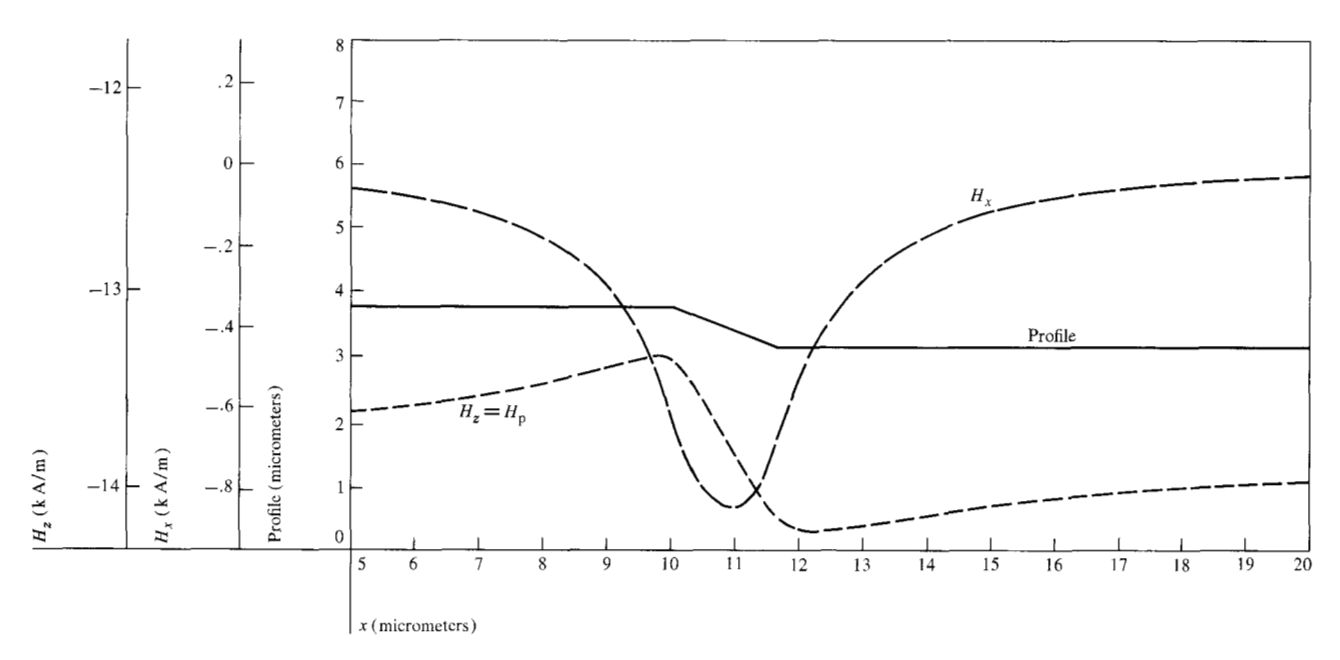


Figure 2 Computation of in-plane field H_x and the field normal to the surface H_z as a function of film thickness for a 20° gradient. The saturation magnetization $M_s = 13.85 \text{ kA/m}$.

and below this value near the slope. When a change in thickness occurs, the magnitude of the z-averaged $H_{\rm p}$ can be greater than $M_{\rm s}$ at some position.

The main features of Fig. 2 are that the gradient of $H_{\rm p}$ is such as to repel a bubble coming from $x=-\infty$ and to attract a bubble from $x=+\infty$ to the bottom of the slope. On the slope, the gradient of $H_{\rm p}$ is in the direction to move the bubble down the slope to the right. This, however, is only one component of the force, and the total picture may change when the other components are included.

Using the computational methods discussed in Appendixes A and B, we compute the force on the bubble as it passes through the gradient region for the case of the isolated bubble. A bias field of 4.94×10^3 A/m, consistent with bubble stability in both the thick and thin regions, was applied. Figure 3 shows the results of such a calculation.

The three parameters (force, energy, and diameter) are shown as functions of the position x of the center of the bubble. The top of the slope is arbitrarily set at $x = 10 \mu m$. A negative force translates the bubble in the -x direction and a positive force in the +x direction. At each point x, the bubble energy is minimized to obtain the stable diameter. We assume that the bubble is being driven by an external force in the +x direction.

As the bubble approaches the slope from left to right, it experiences an increasing repulsive force that peaks at about $2.4 \times 10^2 A/m$. Therefore, the bubble must be

forced over the barrier by an external force until the internal force recedes to zero near the top of the slope. This is a point of unstable equilibrium, as shown by the peak of the energy curve. At this point, the slightest amount of force will move the bubble down the slope, aided this time by the positive internal force. The bubble will then come to rest at the bottom of the slope, a point of stable equilibrium.

Proceeding farther to the right, we see that the external force must overcome the "pull-off" force to push the bubble farther up the energy curve, far to the right. If we had moved the bubble from right to left, all internal forces would have the opposite effect. The bubble would be attracted to the bottom of the slope, and would have to be pushed up the slope and then pulled away to the left. The general result would be that the thinner region would always be at a higher energy than the thicker one, with a metastable state in between. From the Figure it is clear that, when the bubble is on the slope, the two components of Eq. (7) have opposite sign, the net force being the differences between the two and in the direction to push the bubble down the slope opposite the thickness gradient. Although the thicker region is the lowest energy state, for abrupt changes in thickness the bubble must be pushed up the slope.

Note the appreciable change in bubble diameter as the bubble goes through the slope. This fact cannot be neglected because erroneous results are obtained if the diameter is calculated as a fixed quantity.

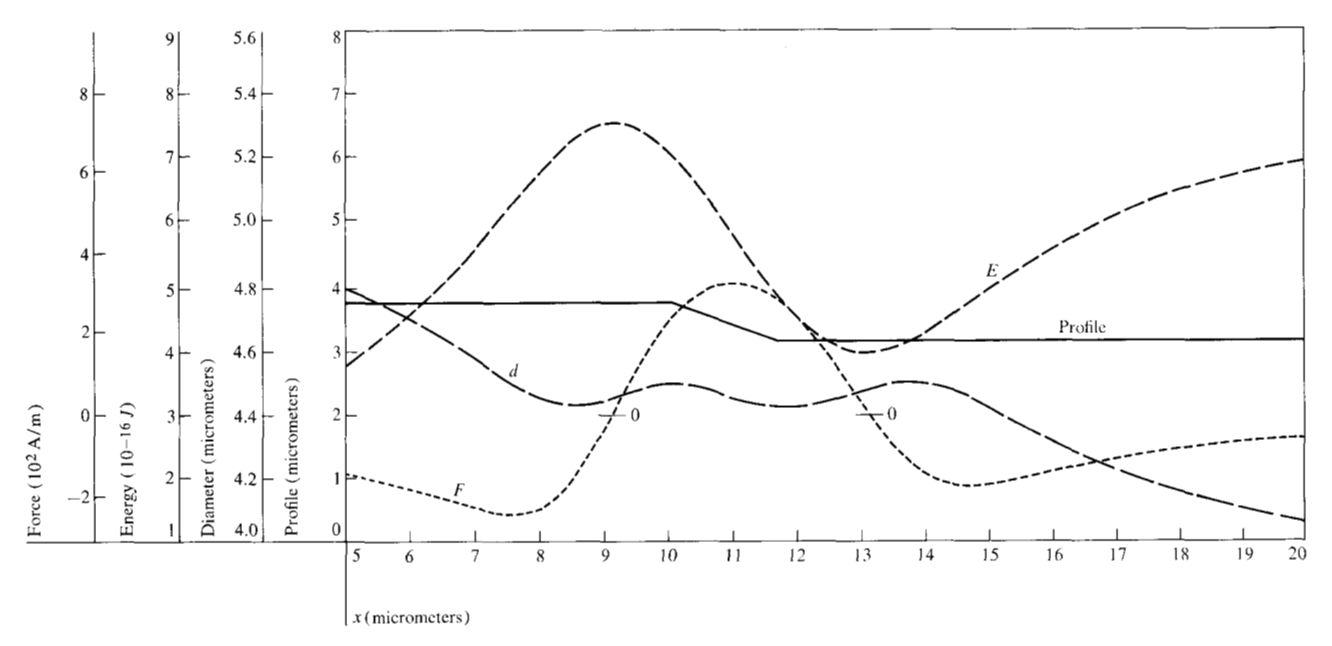


Figure 3 Computation of force energy and diameter as a function of film thickness for a 20° gradient. The force is given as an effective field difference over the bubble diameter. The bias field $H_a = 4.94 \times 10^3 \text{ A/m}$ and $\Delta h = 0.62 \mu\text{m}$. The reduced force is $F_t / \pi r h \mu_0 M_s$.

To complete the model, the gradient field resulting from the current flow in the conductors is computed and is included in the energy calculations. Using these results for various values of conductor current permits the prediction of the external force necessary to overcome the internal force at any position.

To verify the model, a laboratory experiment was performed on ion-milled bubble material with the configuration shown in Fig. 4. Short pulses of current in the conductor overlay position the bubble at points A, B, C, and D. The experiment consists in measuring the minimum drive field required to move the bubble to the various positions. The internal forces can then be deduced from the measurements of the minimum drive necessary for translation. Table 2 compares the experimental results with predicted results in Fig. 3. Points A and D are taken at least 15 μ m away from the slope, and points B and C are located at the top and bottom of the slope, respectively. The predicted results are adjusted to include the coercivity $H_{\rm e}$, which is not included in the model. A value of $(8/\pi)$ $H_c = 79.6$ A/m is used to fit the experimental data.

Acknowledgments

The authors acknowledge the efforts of D. Y. Saiki, who fabricated the ion-milled slopes, and of D. M. Franich, who performed the experimental measurements. The support of B. A. Calhoun and L. L. Rosier during the course of this work is also acknowledged.

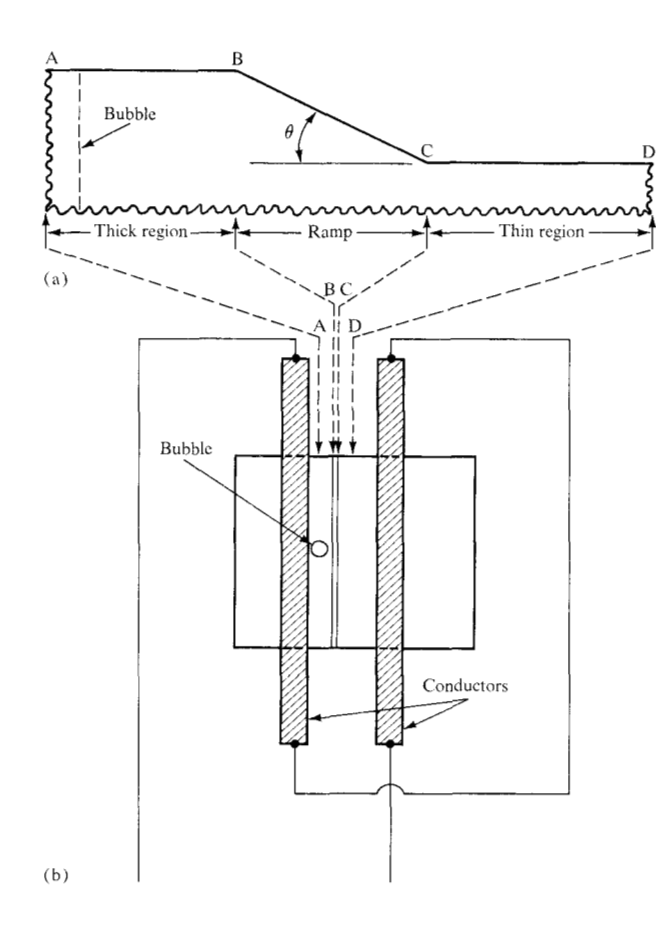
Appendix A: Magnetic field computations for piecewise linear platelet geometry

For purposes of field calculations, the platelet geometry is considered as indicated in Fig. 1. The platelet is infintely long in its y dimension and consists of prescribed plane strips fitted together in a "broken line" arrangement. When the platelet is magnetized with strength M in the +z direction, the resulting negative magnetic charges on the bottom of the platelet and on the strips comprising its top surface. Note that the magnetic charge on an inclined portion of the platelet surface depends on the angle of inclination, Θ , as well as on the strength of magnetization M and is given as $M \cos \Theta$.

The field due to an infinitely long, charged strip may be calculated directly from first principles by integration. Let the charge on the strip be S, its half-width be a, and

Table 2 Test results on ion-milled garnet film, Fig. 4

Positions	Measured force (A/m)	Predicted force (A/m)
$A \rightarrow B$	318	334
$B \rightarrow C$	79.6	79.6
$C \rightarrow D$	270	263
$D \rightarrow C$	23.9	0
$C \rightarrow B$	350	414
$B \rightarrow A$	127	79.6



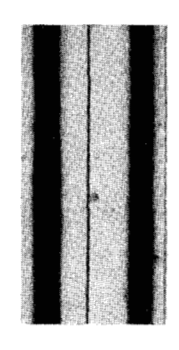


Figure 4 Experimental configuration, showing (a) an expanded sketch of the sample area between the conductors, sectioned through the center of the bubble, and (b) a plan-view sketch of the conductor and bubble positions on the garnet film, scaled to (c) a photograph of the film with the thickness gradient centered between the conductors.

its inclination angle with respect to the x axis be Θ . The x and z components of field are $H_x = S[T \sin \Theta + L \cos \Theta]$ and $H_z = S[-T \cos \Theta + L \sin \Theta] = H_y$, where

$$T = \tan^{-1} \frac{2a(x \sin \Theta - z \cos \Theta)}{x^2 + z^2 - a^2} ,$$

$$L = \ln\left(\frac{1+A}{1-A}\right),\,$$

$$A = \frac{2a(x\cos\Theta + z\sin\Theta)}{x^2 + z^2 + a^2},$$

and x, y are components of distance from the center line of the strip to the field point.

Conducting strips deposited on the platelet surface can provide a current-induced field, which again may be calculated from first principles.

For the purpose of computing the effects of nearneighbor bubbles on the one whose transverse force is under study, the field of a cylindrical bubble (or its dipole approximation) must be calculated. Such field components can again be derived from first principles, resulting in elliptic integrals of the first, second, and third kinds [5]. Reference 6 includes efficient algorithms for calculating such integrals as part of a computer program.

Appendix B: Computation of bubble energy

The internal magnetizing field of the bubble, H_v , can be expressed as $H_v = 2M_sN_v(d/h)$, where $N_v(d/h)$ is the volume-averaged demagnetizing factor for a cylinder of diameter d and height h, and is

$$\begin{split} N_{\rm v} &= 1 + \left(\frac{4d}{3\pi h}\right) \left\{1 - \frac{1}{k^3} \left[(1 - k^2) K(k) \right. \right. \\ &+ (2k^2 - 1) E(k) \left. \right] \right\} \end{split}$$

and tabulated by Brown [7], where

$$k = \frac{d/h}{[(d/h)^2 + 1]^{\frac{1}{2}}}$$

and K(k) and E(k) are complete elliptic integrals of the first and second kinds.

In a flat portion of the platelet the bubble volume and area may be calculated directly from the proper formulas. When all or part of the bubble intersects a part of the gradient on the top surface, the volume and area may be calculated as the sum of contributions from cylindrical fragments with sloping plane tops. Given the volume of the composite bubble, the height of a standard cylindrical bubble of the same volume can be used to calculate an equivalent demagnetizing value $N_{\rm v}$. The energy $\Delta E_{\rm T}$ may then be minimized as a function of bubble diameter d. Given bubble energy as a function of position in the platelet, transverse forces may be calculated by appropriate central differences.

References

- A. A. Thiele, A. H. Bobeck, E. Dellatorre, and U. F. Gianola, "The Energy and General Translation Force of Cylindrical Magnetic Domains," *Bell System Tech. J.* 50, 711 (1971).
 W. F. Druyvesteyn, "Thickness and Magnetization Varia-
- W. F. Druyvesteyn, "Thickness and Magnetization Variation in Magnetic Bubble Materials," J. Appl. Phys. 46, 1342 (1975).

(c)

- 3. J. A. Cape and G. W. Lehman, "Magnetic Domain Structures in Thin Uniaxial Plates with Perpendicular Easy Axis," *J. Appl. Phys.* **42**, 5732 (1971).
- J. Appl. Phys. 42, 5732 (1971).
 4. A. A. Thiele, "The Theory of Cylindrical Magnetic Domains," Bell System Tech. J. 48, 3287 (1969).
- W. F. Druyvesteyn, D. L. A. Tjaden, and J. W. F. Dorleyn, "Calculation of the Stray Field of a Magnetic Bubble, with Application to Some Bubble Problems," *Philips Res. Repts.* 27, 7 (1972).
- 6. R. Bulirsch, "Numerical Calculation of Elliptic Integrals and Elliptic Functions III," *Numerische Mathematik* 13, 305 (1969).
- 7. W. F. Brown, Jr., "Single-Domain Particles: New Uses of Old Theorems," *Amer. J. Phys.* 28, 542 (1960).

Received May 6, 1975

The authors are located at the IBM General Products Division, Monterey and Cottle Roads, San Jose, California 95193.